INTERFACING OF BATTERY WITH A MEDIUM VOLTAGE DC-DC CONVERTER
USING MATLAB/SIMULINK

By

ERMIAS K. GEBREAB

B.S., University of Asmara, 2005

A REPORT

submitted in partial fulfillment of the requirements for the degree

MASTER OF SCIENCE

Department of Electrical and Computer Engineering
College of Engineering

KANSAS STATE UNIVERSITY
Manhattan, Kansas

2013

Approved by:

Co-Major Professor
Dr. Noel Schulz

Approved by:

Co-Major Professor
Dr. Sanjoy Das

Abstract

Electrical power, although convenient form of energy to distribute and use, cannot easily be stored in large quantities economically. Most electrical power generated by utility plants is consumed simultaneously in real time. However, in some cases, energy storage systems become crucial when power generated from sources does not fulfill peak power load demand in a power system or energy storage systems are needed as backup. Due to these reasons, various technologies such as batteries, ultracapacitors (UC), superconducting magnetic energy storage (SEMS) and flywheels are beneficial options for energy storage systems.

Shipboard power systems must use one or more energy storage systems in order to backup the existing power system if locally generated power is unavailable. This will lessen the effect of voltage sags on power quality, and improve system reliability. This report mainly focuses on the design of a Boost DC-DC converter and the integration of that converter with a previously designed battery storage model, as well as the effect of varying loads at the end of the converter.

Table of Contents

List of Figures

Acknowledgements

First of all, I would like to express my gratitude to my academic advisor, Dr. Noel Schulz, for her excellent guidance and immense knowledge. My heartfelt thanks go to my co-advisor, Dr. Sanjoy Das, for his unceasing motivation, advice and support. I would also like to extend my thanks to Dr. Anil Pahwa for his help and for serving on my committee.

I would like to acknowledge the academic and technical support I received from the staff and students of Kansas State University. I would also like to give thanks to the United States Office of Naval Research for their financial support under the DEPSCoR program.

Last, but by no means least, I would like to thank my parents and friends who continuously supported and encouraged me throughout my study period.

Chapter 1 - Introduction

Electrical power systems which generate, transport and supply power in real time have become an integral part of day-to-day life, thereby creating a need for reliable electric power for offices, houses, planes, and ships. The electrical power plants in modern ships have grown in size and complexity with the growing demands on ship size, speed, economy, capabilities, safety, comfort and convenience. Electric power is essential to these; hence, understanding the design of a shipboard power system is crucial for proper functioning. Extensive research has been done to improve the fighting capability and functional effectiveness of modern naval ships.

1.1 Shipboard Power System

A typical shipboard power system is radial with bus tiebreakers to reconfigure it. There are usually three to four generators. Steam turbines, gas turbines or diesel engines are used as prime movers for these generators. The generated 450V, 60Hz three-phase AC generator output is distributed throughout the ship over distances up to several hundred meters. A number of three-phase step down transformers are used at load centers to provide different voltage levels.

A simple model of a shipboard system that contains two generators, four load zones, and two buses is given in [1]. The radial nature of the system is vital for easily determining fault location and isolation and coordinating protective devices. Loads are classified as either vital or non-vital and can be either three-phase or single-phase. Power for vital loads is supplied through two separate paths (normal and alternate supply paths) via automatic bus transfers or manual bus transfers [2].

1.2 Shipboard Storage System

A proper power balance between generators and loads is required for stable and efficient functioning of a power system. In a shipboard power system, though, power to the loads is supplied by generators; there are various reasons as to why an effective energy storage system is required. In some cases, because of supply power's inability to sufficiently satisfy peak power demand in a power system, energy storage systems must serve as additional means of source since the power demand is beyond generator capacity. Another reason is outage. Energy storage devices also could be used to compensate for unbalanced power, if necessary, thereby improve system stability.

Currently, due to their high significance, various technologies are available to store energy on a relatively small scale in electrical, mechanical, chemical, and magnetic form. Energy storage mediums include battery, flywheel, ultracapacitor, fuel cell and super conducting magnetic energy storage. Batteries are commonly used mediums even though they have low service time. They have received prominent attention due to their direct contribution to the advancement of technologies ranging from portable electronics to fuel efficient vehicles. Lithium-based batteries are the most dominant type of rechargeable batteries in many aspects [3].

Ultra-capacitors are oftentimes used as well since they are more capable in easing power inadequacies in power systems especially for quick transition; however, they cannot supply active power. Flywheel energy storage systems are the most recent and promising technology to significantly improve power system stability of shipboard power systems [4] because of the advantages of having high power density, high energy density and long service time.

1.3 DC-DC Switch Mode Converters

In many designs one voltage level must be converted to another level. DC-DC switch mode converters have a wide range application in regulated switch-mode dc power supplies and in dc-motor drive. The DC-DC converter inputs an unregulated dc voltage and outputs a constant or regulated voltage. Hence, switch-mode dc-dc converters are used to convert unregulated dc input into a controlled dc output at a desired voltage level [5]. The basic block diagram of a dc-dc converter is shown in Figure 1.1.
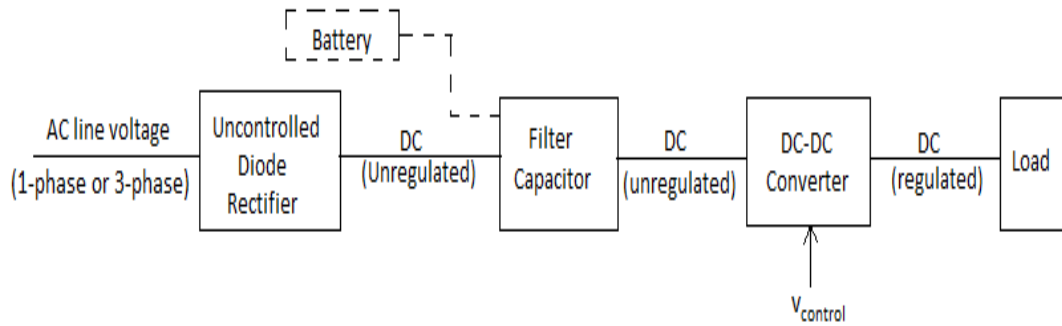
Figure 1.1 DC-DC Converter System [5]

As shown in Figure 1.1, DC-DC converters are generally supplied from an AC network via a rectifier in order to obtain a DC voltage source. Hence, they are used to generate controlled and adjustable DC voltage levels. DC-DC converters are generally classified as Step-down (buck) converter, Step-up (boost) converter, Step-down/step-up (buck-boost) converter, Cuk converter and Full-bridge converter. The basic converter topologies are step-down and step-up, whereas the buck-boost and the Cuk converters are a combination of the two basic topologies and the Full-bridge converter is derived from the step-down converter [5]. The type of converter to be used depends on the specific application. This report concentrates primarily on boost converter because of the need to convert a 400 V input voltage to a 4150 V output voltage.

1.4 Report Objectives

The major objective of this report is to evaluate and modify a previously designed battery model, design a DC-DC boost converter and interface the battery and converter with a load. First, the report discusses work in relation to storage models and converters, including various equivalent electrical circuit models that can accurately predict behavior of electrochemical batteries. The battery model used for this report is a simplified model. Complex models can be used if a high level of accuracy is required. Secondly, a presentation of a design and implementation of a DC-DC boost converter that converts a 400 V supply to 4150 V at the output and result will be offered. Finally, the battery, boost converter and load are integrated into one design and the results of the simulation are presented. The models are designed using MATLAB/Simulink.

Chapter 2. Literature Review of Related Works

In the previous chapter, the design significance of both an accurate battery model and application-oriented DC-DC boost converter were discussed. Over the past few years, extensive research has been undertaken in relation to storage models and converters. The next chapter discusses the achievements of previous researchers.

2.1 Storage Models

With varying degrees of complexity, a variety of models, exist that predict battery behavior to varying degrees of accuracy. The battery model used in this report, which was developed by another student, is based on [6]. The reference paper discussed the modeling of a mechanical-electrochemical lithium-ion battery for an electric scooter application. Dynamic performance prediction of the mechanical-electrochemical model was found to be realistic and matching with the expectations. For a better understanding of lithium-ion batteries, wide ranges of research has been done on developing battery models for different applications and are discussed below.

In [7], L. Gao et al presented a complete dynamic model of a lithium ion battery that accounted for nonlinear equilibrium potentials, rate and temperature dependencies, thermal effects and response to transient power demand. The model was designed in such a way that modifications to fit data from other batteries would be simple and also easily extended for different temperature ranges and current rates. The model attempts an intermediate approach by trying to gain enough accuracy on electrical and thermal properties of the battery while simultaneously avoiding detailed analysis of internal electromechanical processes. To simplify the design the model was coded in Virtual Test Bed computational environment that enables a systematic handling of nonlinearities in model equations.

Chen and Mora [8] proposed a battery model capable of predicting battery runtime and I-V performance accurately and intuitively. The model was implemented in the Cadence environment. The only weakness of the model was neglecting the effects of self-discharge, cycle number and temperature based on the assumption of having low self-discharge rates, long cycle life and constant temperature. The final simulation result of the model was validated with experimental data on polymer Li-ion batteries. The simulation result was very close to experimental data on polymer Li-ion batteries, thus indicating the proposed battery model's accurate prediction of runtime and voltage.

In another paper [9], a new design of lithium-ion battery model using MATLAB/Simulink was discussed and presented. Although, the simulation model design is based on [8], consideration of temperature effect and capacity fading on battery dynamics is added. Consideration of these significant parameters is justified by previous works of [7, 10] and [11, 12, 13]. For validating purposes, results of dynamic simulations of the model were compared with data found by previous studies. After comparing simulations with the data, it was found that battery dynamics were strongly affected by charging/discharging rates, temperature and capacity fading factors. The data verified that the developed model can reflect dynamic output characteristics of a lithium-ion battery and also was able to evaluate battery performance under several operating conditions.

2.2 DC-DC Converters

DC-DC converter is an electrical circuit whose purpose is to provide varying voltage levels that are different than supplied voltage. DC-DC converters are used in order to provide the required voltage level efficiently. Various DC-DC converter models are established providing different operating characteristics depending on the required application. In this section, few achievements of previous researchers will be discussed.

In [14], the design of a DC-DC converter for a PV array is conceptualized and simulated in a circuit that utilizes solar energy for driving high voltage loads. The main purpose was to step-up an input voltage of 17.2 V, obtained from a solar panel, to 325 V dc by the use of multiple boost converters in cascade. Since the proposed system deals with solar panels which have very low output voltage, cascading of the converters is essential in order to achieve a large gain. Prior to [14], little discussion occurred on low-input power converters. However, in [15], a study was conducted on different circuit topologies for power coming from a solar cell. Problems resulted since the startup wasn't handled in a practical method. Hence, [14] has tried to address the previously mentioned problem in a simple and effective manner. The circuit was simulated on MATLB/Simulink.

As a continuation of previous study, a DC-DC converter that employs the voltage lift technique is presented in [16], aimed at improving output voltage of two topologies developed for extra-high voltage applications. The objective was to increase gain of the converters so as to achieve a stage-by-stage increase in output voltage. The paper discussed and analyzed a new series of DC-DC converter topologies. In one of the topologies, three additional stages of inductor and capacitor are incorporated with the basic circuit. The ripple is filtered out and a constant output voltage is maintained due to capacitors that are connected in parallel. The second

topology that was analyzed has additional voltage lift components. The results determined that the proposed converter provides higher power voltage. The paper presented the operation and mathematical analysis of both topologies. Both converter topologies were modeled in MATLAB7 using Simulink toolbox.

Another boost converter design and simulation approach that considered both open loop system and closed system is provided in [17]. The low voltage of PV arrays and fuel cells demands high step-up and high efficiency DC-DC converters. The paper presented circuit models of both open loop and closed loop controlled systems using blocks of Simulink. They utilized maximum power point tracker (MPPT) technique in a photovoltaic energy conversion system in order to achieve maximum power from the solar array, regardless of weather or load conditions. It also presented a detailed comparison of many available tracking algorithms. Simulation of an open loop and closed loop controlled boost converter system was performed using Matlab. Results are presented. The results indicate that a constant voltage was maintained by the closed loop system and the boost converter was able to step-up the voltage level to the required level.

A novel technique of incorporating a DC-DC boost converter in an AC-DC-AC conversion system is proposed in [18]. The paper's main emphasis was on the behavior of marine and tidal current converters and analysis of the proposed conversion system performance. It accounts for the main differences between wind power and marine/tidal current energy and, consequently, a maximum power point tracker (MPPT) is considered. Including a DC-DC converter in the proposed conversion system helped regulate and maintain the inverter DC input voltage within a suitable value, thus enabling the PWM inverter to transform DC voltage to desired load voltage and frequency. The proposed conversion system avoids consideration of the

discontinuous conduction mode (DCM) to eliminate a faulty operation of the DC-DC converter. It presented the architecture of the conversion system, description of system modeling and control strategy, and provided the simulated model and the simulation results using MATLAB/Simulink. The results demonstrate that the DC-DC boost converter has improved system performance with the ability to regulate load voltage and frequency.

2.3 Summary

In the past two decades, many techniques have been developed in modeling storage and converter models, ranging from low voltage to high voltage. These models and designs are typically based on specific application and, therefore considered several assumptions and targets. Therefore, this report analyzes and discusses the design and modeling of a DC-DC converter for a MVDC shipboard power system and interfacing of the converter with a battery and load.

Chapter 3. Design of DC-DC Converter

Because of their high efficiency and capability to provide step-up, step-down or inverter output, switching regulators are more preferred than linear regulators in designing converters. In switching regulator circuits, semiconductor switches contribute greatly to controlling dynamic transfer of power from input to output quickly. A ripple is added to the output voltage because of switching action. While designing switching regulators, the output requirement is a dc voltage with a minimum addition of ac ripple. The most widely used technique for controlling output voltage is pulse width modulation (PWM) because it helps maintain a constant switching frequency and varies the duty cycle. The next section discusses various converter topologies and their operation.

3.1 Buck (Step-down) Converter

As the name implies, the buck converter is used for step-down operation and has a wide range of application in regulated power supplies and dc-motor speed control. The basic circuit of a buck converter is shown in Figure 3.1.
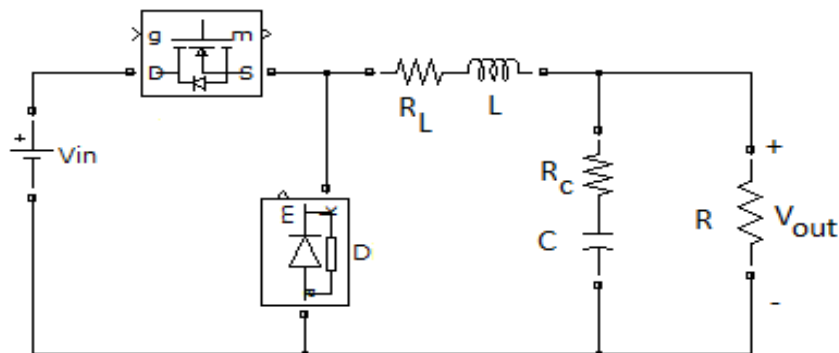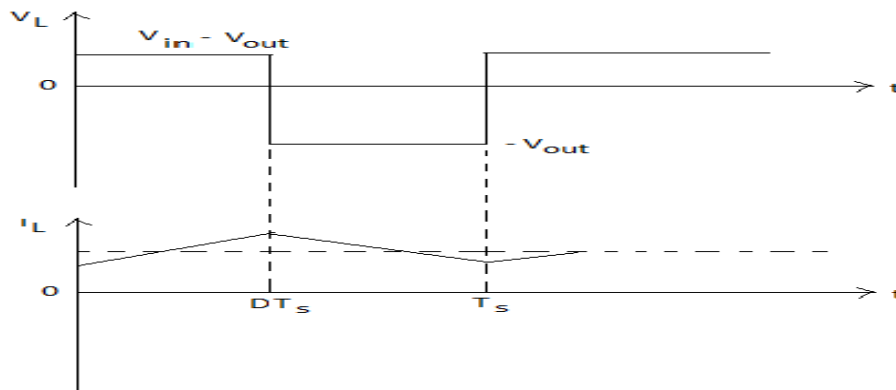
Figure 3.1 Buck DC-DC Converter [Adapted from [5]]

When the transistor is on, the input voltage appears across the inductor, current increases linearly, and the capacitor becomes charged. When the transistor is off, the voltage across the inductor is reversed. However, since current in the inductor cannot change instantaneously, it begins to decrease linearly. The capacitor is again charged by energy stored in the inductor. The two modes of operation are continuous and discontinuous. In continuous mode, the inductor current never reaches zero. In discontinuous mode, the inductor current reaches zero in one switching cycle and the regulate output voltage has no linear relationship with the input voltage, as in continuous conduction mode operation.

Analyzing the inductor current waveform determines the relationship between output and input voltage in terms of duty cycle. Duty cycle is defined as the ratio of switch on time to the reciprocal of switch frequency. In a well-designed converter, the main objective is to minimize the percentage of ripple at the output. As a result, output voltage can be approximated by its DC component [5]. Inductor current is found by integrating the inductor voltage waveform. The waveforms of the inductor voltage and current for a buck converter are shown in Figure 3.2.

Figure 3.2 Steady-state inductor voltage and current waveform of Buck Converter [Adapted from [5]]

In steady state, the net change in inductor current is zero, according to the principle of inductor volt second balance. The inductor voltage is given by V_L

$$VL = L \frac{di_L}{dt} \tag{3.1}$$

Where: V_L = voltage across inductor (V)

L = Inductor (H)

i_L = inductor current (A)

Integration over one complete switching period yields,

$$iL(Ts) - iL(0) = \frac{1}{L} \int_0^{Ts} VL(t)dt \tag{3.2}$$

Where: T_s = switching period

The left hand side of the above equation is zero. Hence, equation (3.2) can be written as

$$\int_0^{Ts} VL(t)dt = 0 \tag{3.3}$$

Alternatively, total area under $V_L(t)$ waveform over one switching period must be zero. Area under the $V_L(t)$ curve is given by

$$A = \int_0^{Ts} VL(t)dt = (Vin - Vout)(DTs) + (-Vout)(D'Ts) \tag{3.4}$$

Where: D = Duty cycle

D' = Complement of duty cycle (1-D)

V_{in} = Input voltage

V_{out} = Output voltage
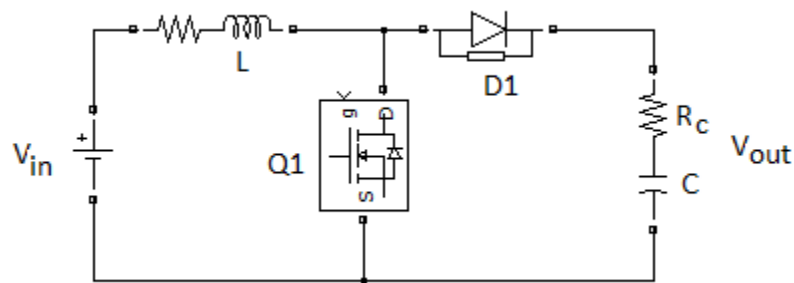
The average value of inductor voltage is given by,

$$< VL > = \frac{A}{Ts} = D(Vout - Vin) + D'(-Vout) \tag{3.5}$$

By equating $<V_L>$ to zero and using the relation D+D'=1, and solving for V_{out} yields

$$Vout = D.Vin \tag{3.6}$$

3.2 Boost (Step-up) Converter

The circuit topology of a boost converter, capable of producing a dc output voltage greater in magnitude than the dc input voltage, is shown in Figure 3.3.

Figure 3.3 Boost DC-DC Converter [Adapted from [5]]

The current in the inductor L increases linearly when the transistor Q1 is on, while the capacitor C simultaneously supplies the load current and is partially discharged. When the transistor Q1 is off in the second interval, the diode is on and the inductor L supplies the load and also recharges the capacitor C. The steady state inductor current and voltage waveforms are shown in Figure 3.4.
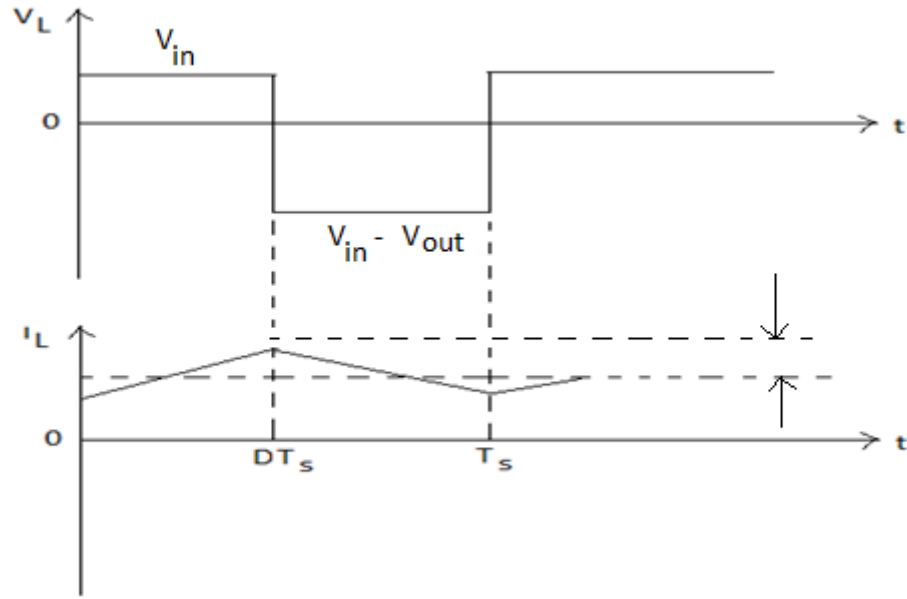
Figure 3.4 Steady-state inductor voltage and current waveform of a Boost Converter [Adapted from [5]]

Applying the inductor volt balance principle to obtain the steady state output voltage equation yields

$$Vin * Ton + (Vin - Vout) * Toff = 0 \qquad (3.7)$$

Where: T_{on} = Switch on time

T_{off} = Switch off time

$$\frac{Vout}{Vin} = \frac{1}{1-D} \qquad (3.8)$$

As seen in the equation of 3.8, the output voltage of the converter is greater than the input voltage; hence, the input current that is also the inductor current is greater than the output current. In practice, the inductor current flowing through, semiconductors Q1 and D1, the inductor winding resistance becomes very large and with the result being that component non-idealities may lead to large power loss. The inductor current becomes very large as the duty

14

cycle approaches one and, therefore, these component non-idealities lead to large power loss. Consequently, efficiency of the boost converter decreases rapidly at high duty cycles.
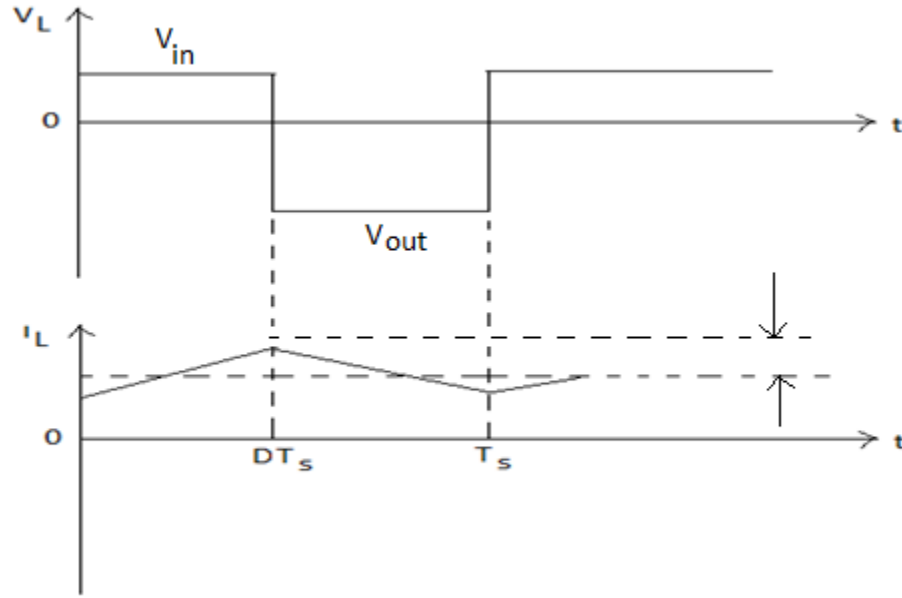
3.3 Buck-Boost Converter

The arrangement for a buck-boost converter capable of producing a dc output voltage either greater or smaller in magnitude than the dc input voltage is shown in Figure 3.5.
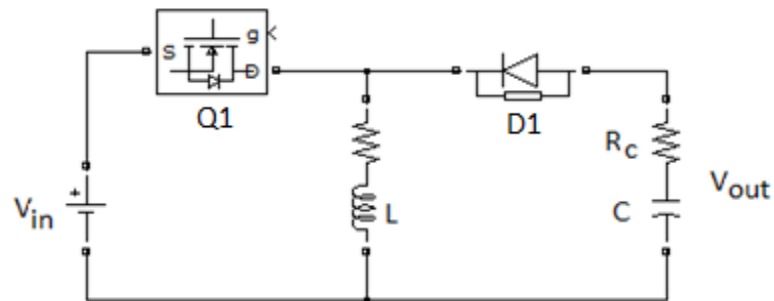
Figure 3.5 Buck-Boost DC-DC Converter [Adapted from [5]]

When transistor Q1 is on, input voltage is applied across the inductor and the current in inductor L rises linearly. At this time, the capacitor C; supplies the load current; and is partially discharged. During the second interval, when the transistor is off, voltage across the inductor reverses in polarity and the diode conducts. During this interval, energy stored in the inductor supplies the load and, recharges the capacitor. The steady inductor and voltage waveforms are shown in Figure 3.6.

Figure 3.6 Steady-state inductor voltage and current waveform of a Buck-Boost Converter [Adapted from [5]]

Applying the inductor volt balance principle to find the steady state output voltage equation yields

$$Vin * Ton + Vout * Toff = 0 \qquad (3.9)$$

$$\frac{Vout}{Vin} = -\frac{D}{1-D} \qquad (3.10)$$

Since the duty cycle (D) can vary between 0 and 1, output voltage can be lower or higher than the input voltage in magnitude but opposite in polarity.

3.4 Cuk Converter

Cuk converters are obtained by cascading a buck and boost converter. As previously mentioned, the transfer of energy between input and output in buck, boost, and buck-boost converters takes place with the help of an inductor, and analysis is based on voltage balance

across the inductor. However, Cuk converter utilizes capacitive energy transfer and analysis is based on current balance of the capacitor. The arrangement of a Cuk converter is shown in Figure 3.7.
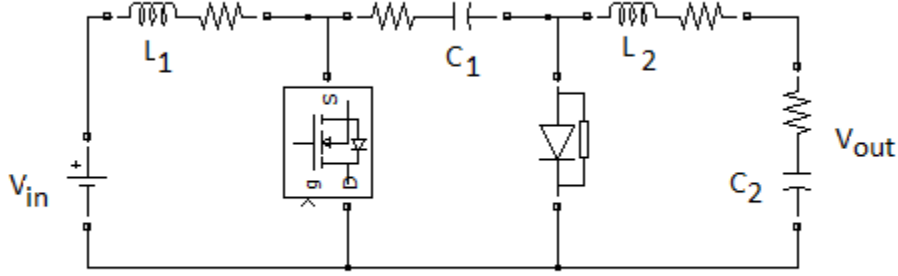
Figure 3.7 Cuk DC-DC Converter [Adapted from [5]]

When the diode is on, the capacitor is connected to input through L_1 and source energy is stored in the capacitor. During this cycle the current in C_1 is I_{in}. When transistor Q_1 is on, energy stored in the capacitor is transferred to the load through the inductor L_2. During this cycle, the current in C_1 is I_{out}. The capacitive charge balance principle is used to obtain steady state solution.

$$I_{in} * T_{off} + (-I_{out}) * T_{on} = 0 \qquad (3.11)$$

$$\frac{I_{out}}{I_{in}} = \frac{(1-D)}{D} \qquad (3.12)$$

Then, using the power conservation rule

$$\frac{V_{out}}{V_{in}} = -\frac{D}{(1-D)} \qquad (3.13)$$

17

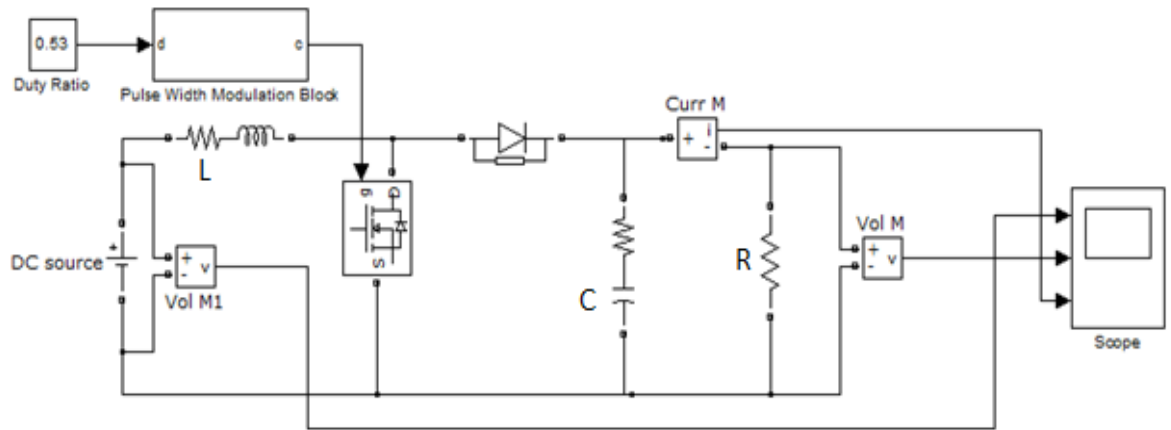## 3.5 Design of a Low Voltage DC-DC Boost Converter

System modeling is possibly the most important phase in any form of system control design work. The choice of a circuit model depends on objectives of the simulation. Designing converters involves solving difficult general nonlinear equations, hence all governing equations are put together in block diagram form and then simulated using Matlab's Simulink program. Simulink solves these nonlinear equations numerically; and provides a simulated response of the system dynamics.

Boost converter is used to obtain a load voltage higher than the input voltage V_{in}. The values of L and C are chosen based on requirements of output voltage and current. When the switch is ON, the inductor L is connected across the supply. The inductor current I_L rises and the inductor stores energy during the ON time of the switch, T_{on}. When the switch is off, the inductor current I_L is forced to flow through the diode D and load for a period, T_{off}. The current tends to decrease, resulting in a reversal of polarity of the induced EMF in L. Therefore, voltage across the load is given by:

$$Vout = L\left\{\frac{dl}{dt}\right\} \tag{3.14}$$

The circuit that models the basic operation of the boost converter is shown in Figure 3.8. That circuit is needed to design a 24V to 48V DC-DC boost converter.

Figure 3.8 Simulation Model of a Low Voltage DC-DC Boost Converter

The large capacitor connected across the load provides a continuous output voltage, and the diode prevents any current flow from capacitor to the source. In the design, the average output of the DC-DC converter is controlled by pulsed width modulating the duty ratio. The converter output voltage is measured and compared with its reference value with in a PWM controller, and its design on Simulink is shown in Figure 3.9.
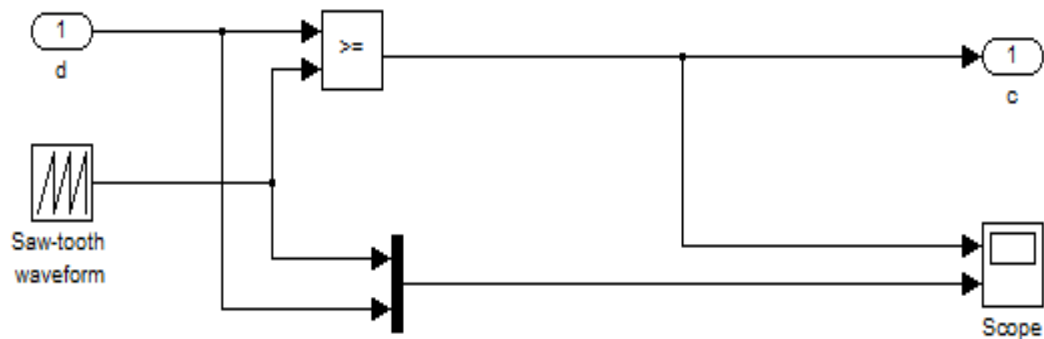
Figure 3.9 PWM Subsystem of a Low Voltage DC-DC Boost Converter

In the design process, although the switching circuit theoretically can work with a large range of frequencies, a switching frequency of 100 KHz is chosen because as the frequency

19

increases the circuit requires less inductance and capacitance. Hence, in order to get the desired output, different values of capacitance and reactance were considered while changing the switching frequency simultaneously.

The final design parameters of the model are found to be: V_{in} = 24V, V_{out} = 48V, C = 220µF, L = 161.95µH, f_s = 100KHz,

PWM = 100e3

$$\frac{Vout}{Vin} = \frac{1}{1-D} = \frac{48}{24}$$

Therefore,　　D = 0.5

3.6 Design of a Medium Voltage DC-DC Boost Converter

The operational principles and analysis used in designing a medium voltage DC-DC boost converter are similar to design procedures of a low voltage DC-DC converter. The circuit that models the boost converter shown in Figure 3.10 had a switching period of T and duty cycle of D calculated from the input and output voltages.
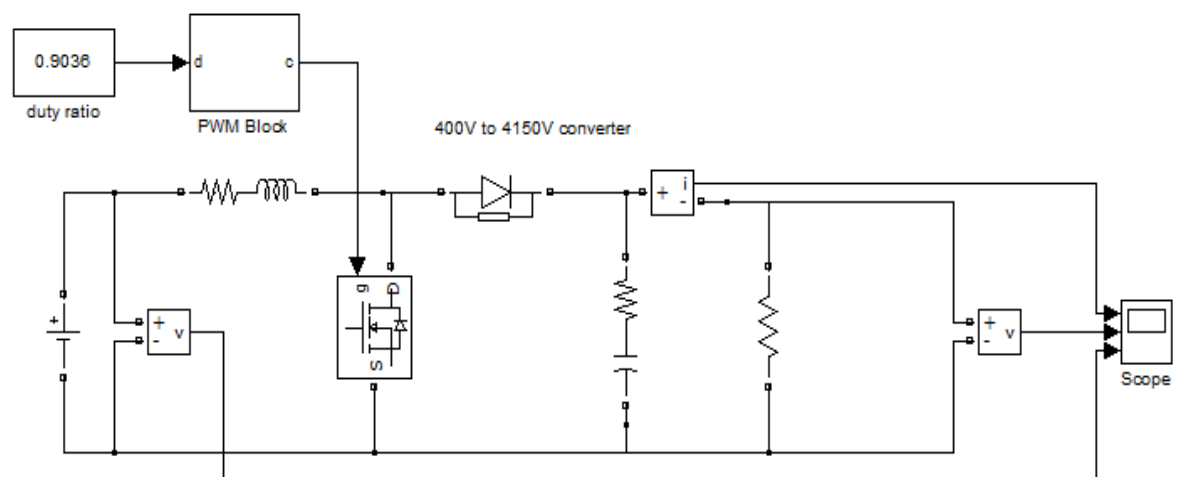
Figure 3.10 Simulation Model of a Medium Voltage DC-DC Boost Converter

3.6.1 Operational Principles and Assumptions

In designing and analyzing the circuit of the boost converter, the following assumptions are considered [19]:-

- When the switch is on, the drop across it is zero and the current through it is zero.

- The diode has zero voltage drops in conducting state and zero current in reverse-bias mode.

- The time delay in turning on and off the switch and the diode are negligible.

- The inductor and capacitor are lossless.

- The response of the circuit is periodic. The value of inductor current at the start and end of a switching cycle is the same. The net increase in inductor current over a cycle is zero.

- The switch is made ON and OFF at a fixed frequency; let the period corresponding to the switching frequency be T. Given the duty cycle is D, the switch is on for a period equal to DT; and off for a time interval equal to $(1 - D)T$.

- The inductor current is continuous and greater than zero.

- The capacitor is relatively large. The RC time constant is so large; that, when the switch is ON and OFF, changes in capacitor voltage can be neglected for calculating change in inductor current and average output voltage. The average output voltage is assumed to remain constant.

- The source voltage V_{in} remains constant.

3.6.2 Pulse Width Modulation (PWM)

In designing DC-DC converters, control of average output voltage (V_{out}) must be equal to a specifically desired level of voltage. This can be achieved in DC-DC converters by controlling the switch on and off durations (T_{on} and T_{off}). Hence, average output voltage depends on T_{on} and T_{off}. One way of controlling output voltage is by switching at a constant frequency and adjusting the on-duration of the switch in order to control average output voltage. This technique is called pulse-width modulation switching, and the switch duty ratio D, which is defined as the ratio of on-duration to the switching time period, is varied.

In PWM switching, which employs constant switching frequency, control of the state of the switch is done by the switch control signal which is generated by comparing a signal level control voltage having a repetitive waveform [20]. Amplifying the difference between actual output voltage and its desired value helps in obtaining the control voltage signal. The switching frequency obtained from the repetitive waveform is kept constant and is chosen to be in a few kilohertz to a few hundred kilohertz range. The block diagram of a pulse-width modulator (PWM) and comparator signals are shown in Figure 3.11 and Figure 3.12, respectively.

The switch duty ratio can then be expressed as

$$D = \frac{T_{on}}{T_s} = \frac{v_{control}}{V_{st}} \tag{3.15}$$
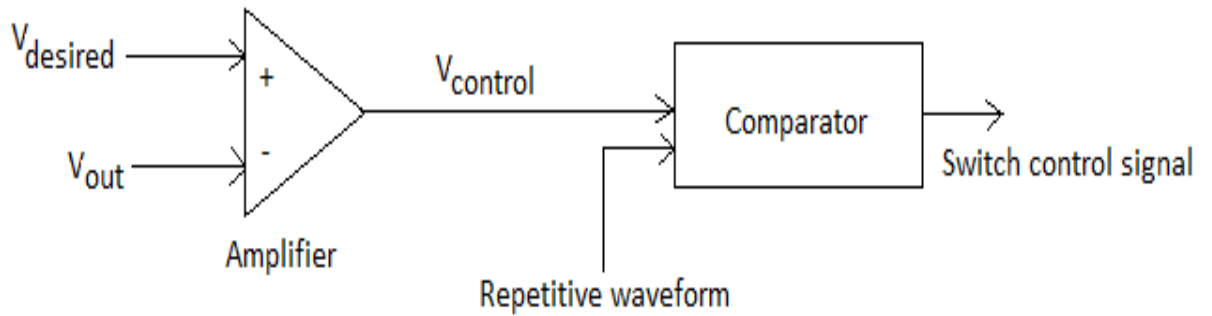
Figure 3.11 Block Diagram of a PWM [5]
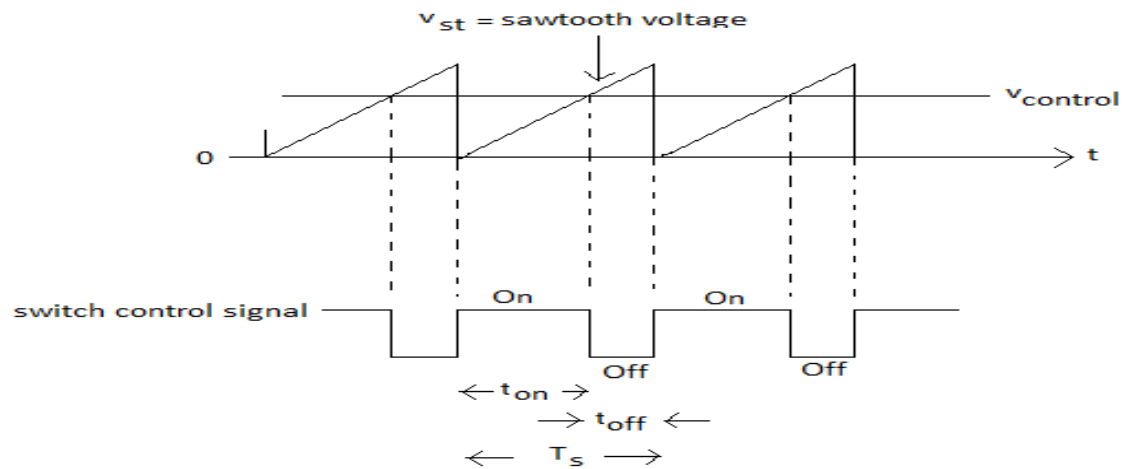
Figure 3.12 Comparator Signals [5]

In the design, as in case of low voltage converter, the average output of the DC-DC converter is controlled by pulsed width modulating the duty ratio. The converter output voltage is measured and compared with its reference value with in a PWM controller, and design of the PWM in Simulink is shown below.
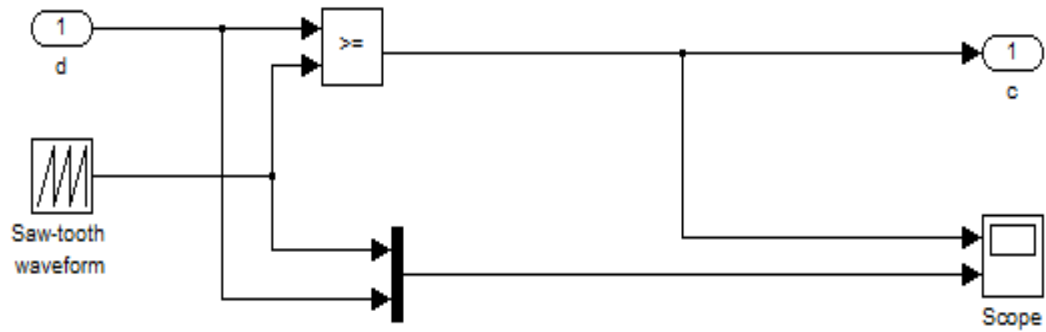
Figure 3.13 PWM Subsystem of a Medium Voltage DC-DC Boost Converter

The desired output voltage is 4150 V and the input voltage is 400 V. Hence,

$$\frac{Vout}{Vin} = \frac{1}{1-D}$$

$$\frac{4150}{400} = \frac{1}{1-D}$$

$$D = 0.9036$$

Value of the inductor is obtained from

$$L = \frac{Vin * D}{fs * \Delta Iout} \tag{3.16}$$

Where: L = inductance of inductor (H)

D = Duty cycle

f_s = Switching frequency (Hz)

ΔI_{out} = current ripple factor (CRF) whose typical value is 20-30%. Therefore,

24

$$L = \frac{400 * 0.9036}{1e5 * 24.16}$$

$$L = 0.1496 \ mH$$

During the design process, different values of switching frequencies (f_s), typically between 200 kHz and 2 MHz, were considered. When higher values of switching frequencies were used the values of the inductance and capacitances were reduced. For this specific design, a switching frequency of 100 kHz is selected in order to achieve the desired output and the inductance and capacitance of the inductor and capacitor are determined based on this value. And value of the capacitor is determined from

$$C = \frac{D * Ts}{R * (\frac{\Delta Vout}{V})}$$

$$C = 0.05 * 34.34$$

$$C = 5.26 \mu F$$

3.7 Simplified Battery Model

As one of the most widely used types of storage devices, a wide range of equivalent circuit models of batteries exist that differ in complexity and predictability. Complex battery

models can predict electrochemical behavior accurately but at the cost of simulation time and memory [21]. Electrical circuit of the battery model used in this report and its equivalent model in Matlab/Simulink are shown in Figure 3.14 and Figure 3.15, respectively.
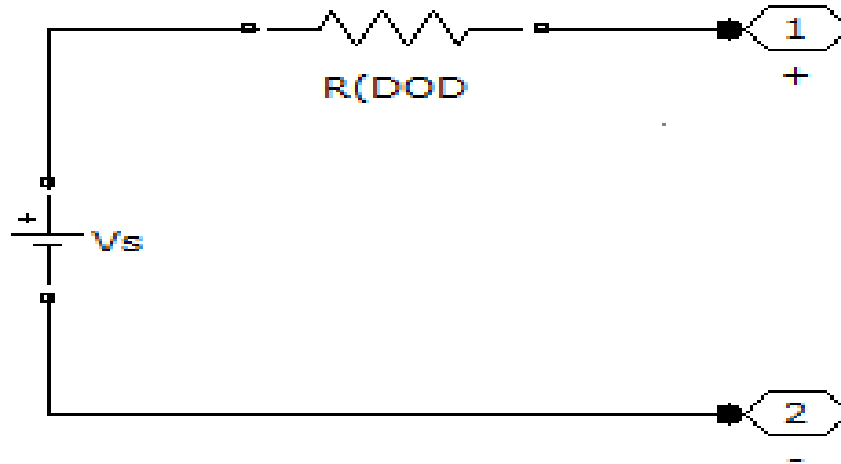
**Figure 3.14 Equivalent Electrical Circuit of a Battery Model**
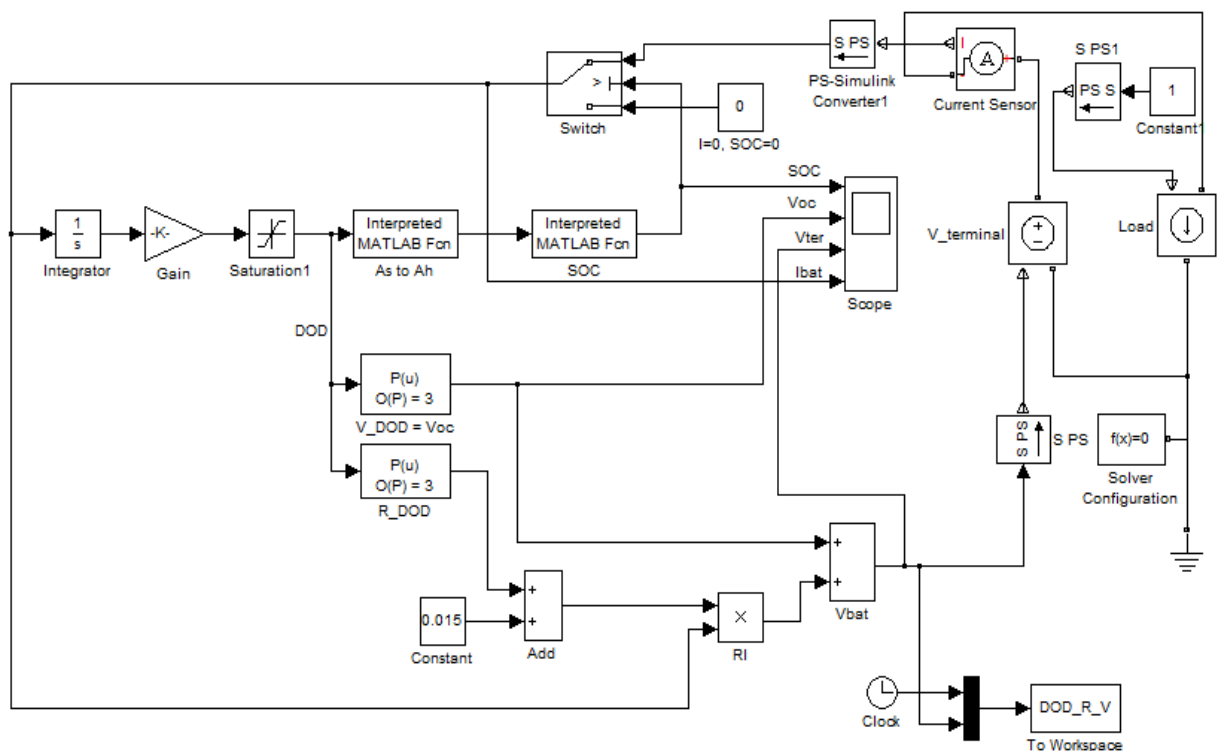
**Figure 3.15 Matlab/Simulink Implementation of the Circuit**

3.8 Load

In designing the DC-DC low voltage boost converter, a single resistance is connected in parallel to the capacitor, resulting in, desired output voltage at the output terminal. However, in designing the medium voltage DC-DC boost converter, resistances must be added in parallel in order to achieve desired output voltage. For this particular design, different values of resistances of low value were initially considered and later were increased depending on the output voltage results of the simulation. A resistance of 1000Ω was found to be suitable to get the desired output. To obtain a 1000Ω of load, four resistances, as shown in Figure 3.1, are connected in parallel to each other, and switches are used to control connectivity of each resistance in the circuit. The load is modeled in Simulink and shown in Figure 3.16.
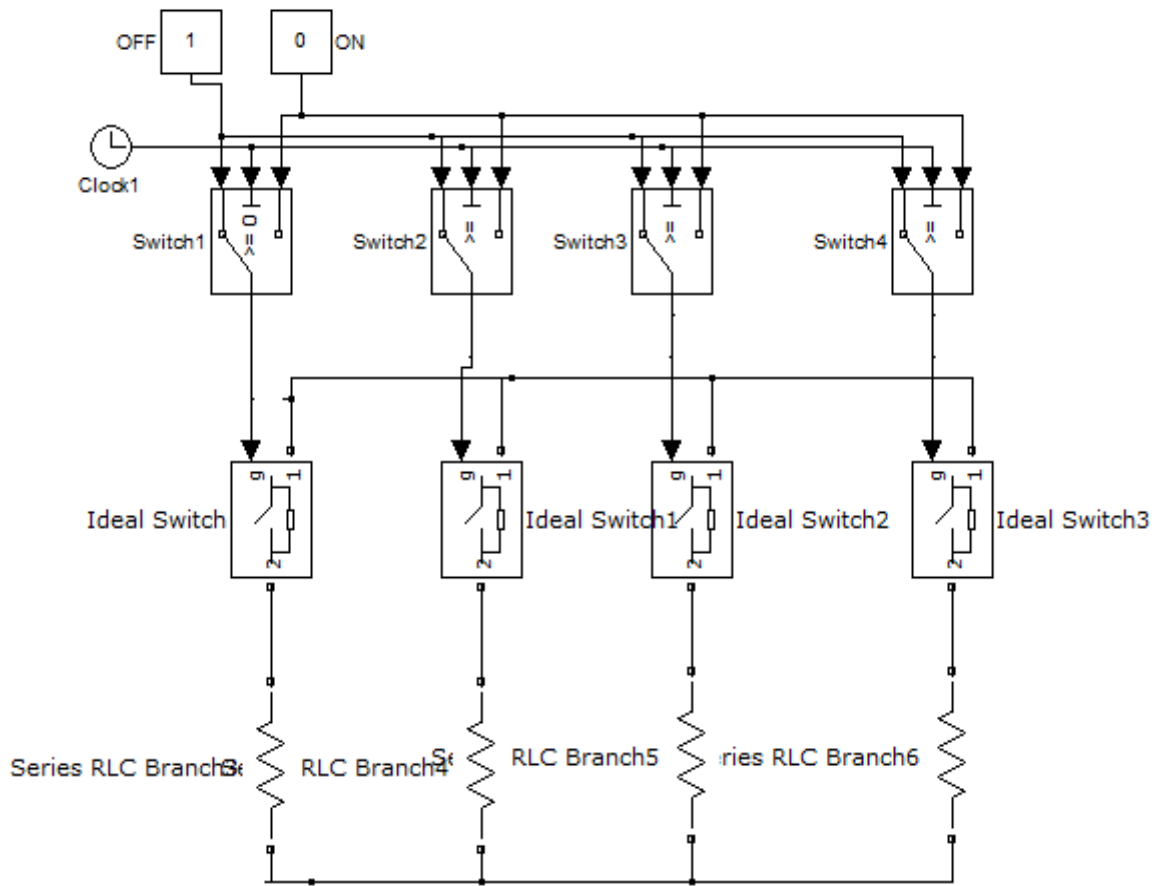
Figure 3.16 Simulation Model of the Load

## 3.9 Merging the DC-DC Converter with the Load

The next step, after designing the DC-DC boost converter and modeling the load in Simulink, was to interconnect the converter with the load and verify the desired output voltage. The Simulink model of the combination of the converter and load is shown in Figure 3.17.
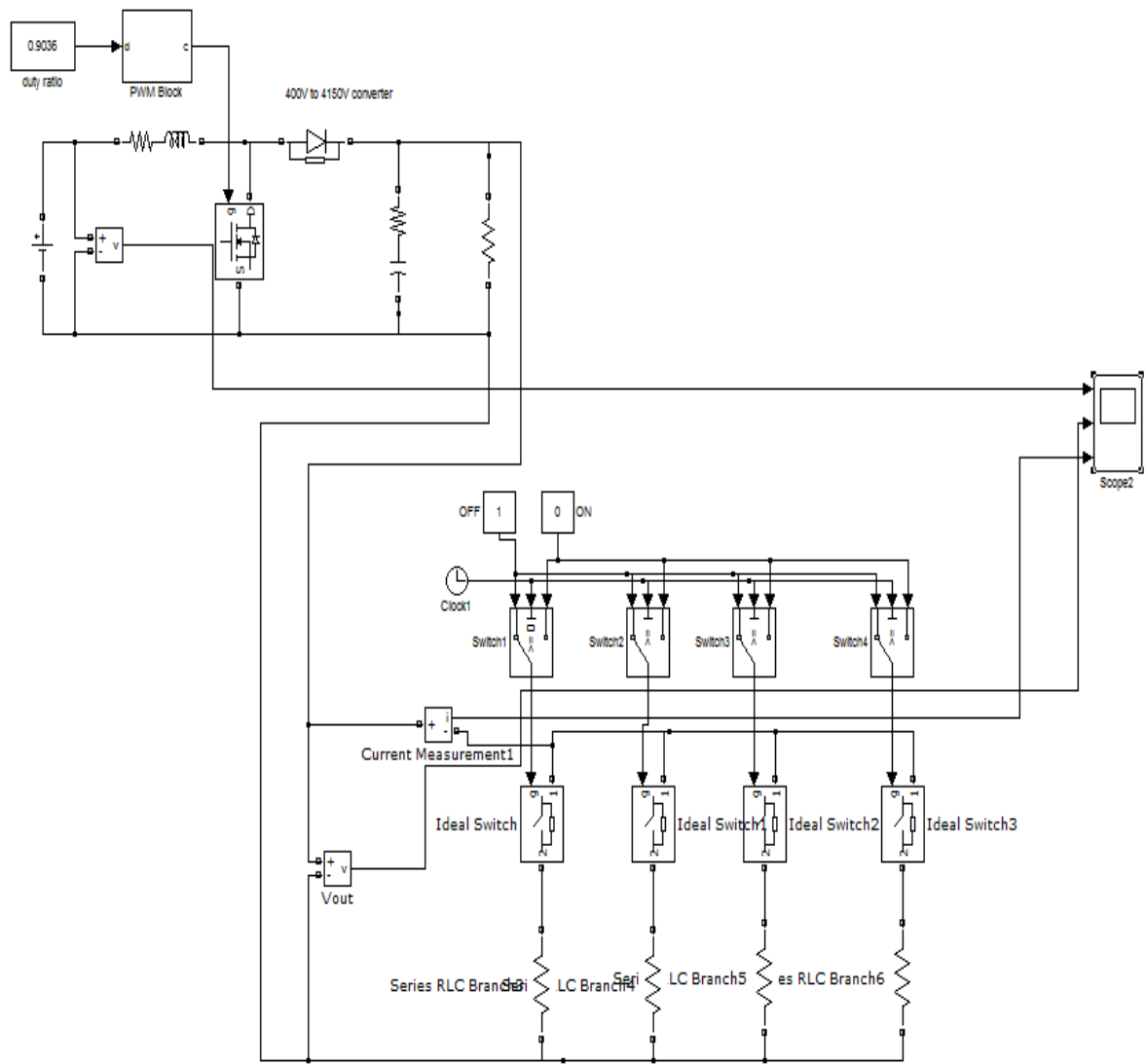
Figure 3.17 Simulation Model of the Converter and Load

3.10 Merging the Battery, DC-DC Converter and the Load

The final step of the design process was to interface the battery, DC-DC converter and the load together and verify results of the simulation. The simulation model of the whole model is shown in Figure 3.18.
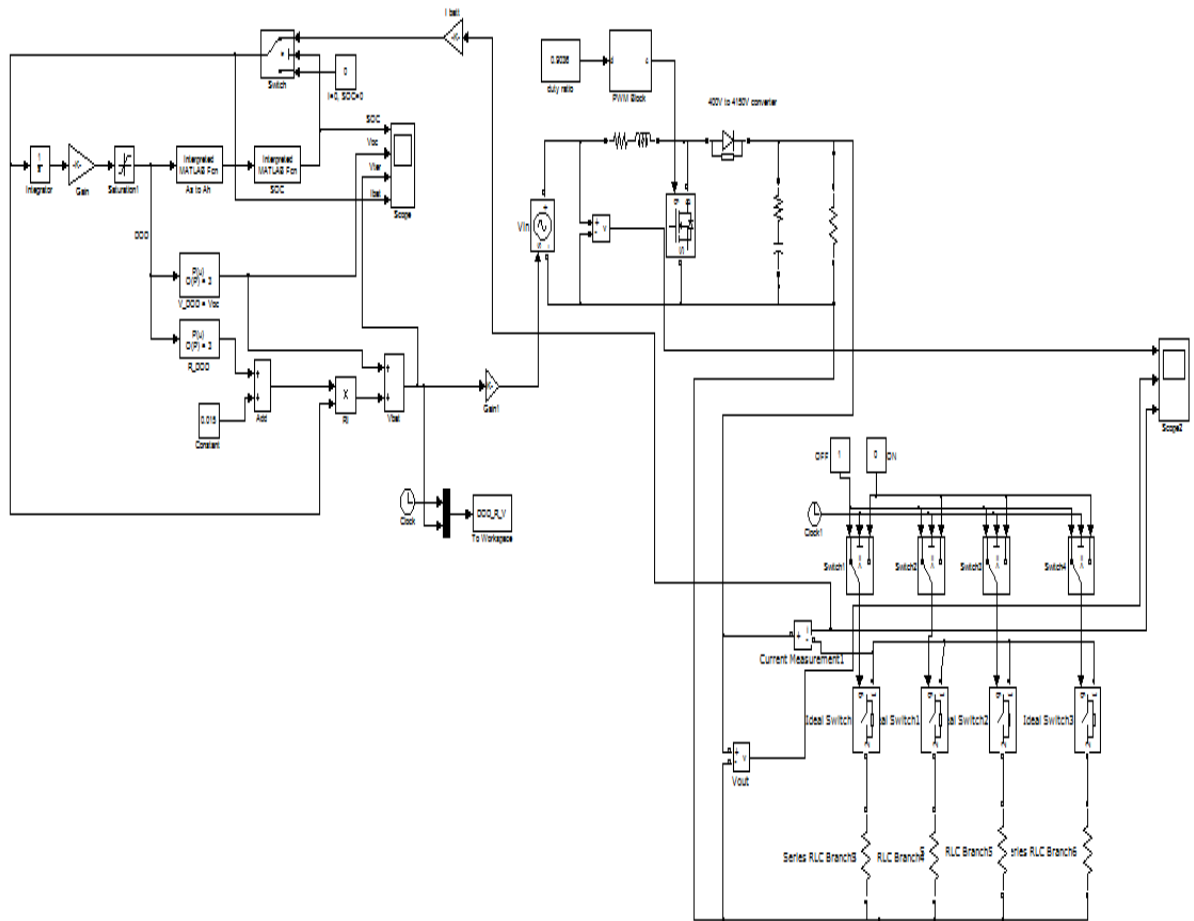
Figure 3.18 Simulation Model of the Battery, Converter and Load

Chapter 4. Results and Summary

4.1 Simulation Results of the Low Voltage DC-DC Converter

Results for this specific design of low voltage DC-DC converter were obtained using the Simulink and are presented in Figure 4.1. As shown, simulated results are in close agreement with expected theoretical results. Expected output voltage at the output terminal of the circuit was 48 V.
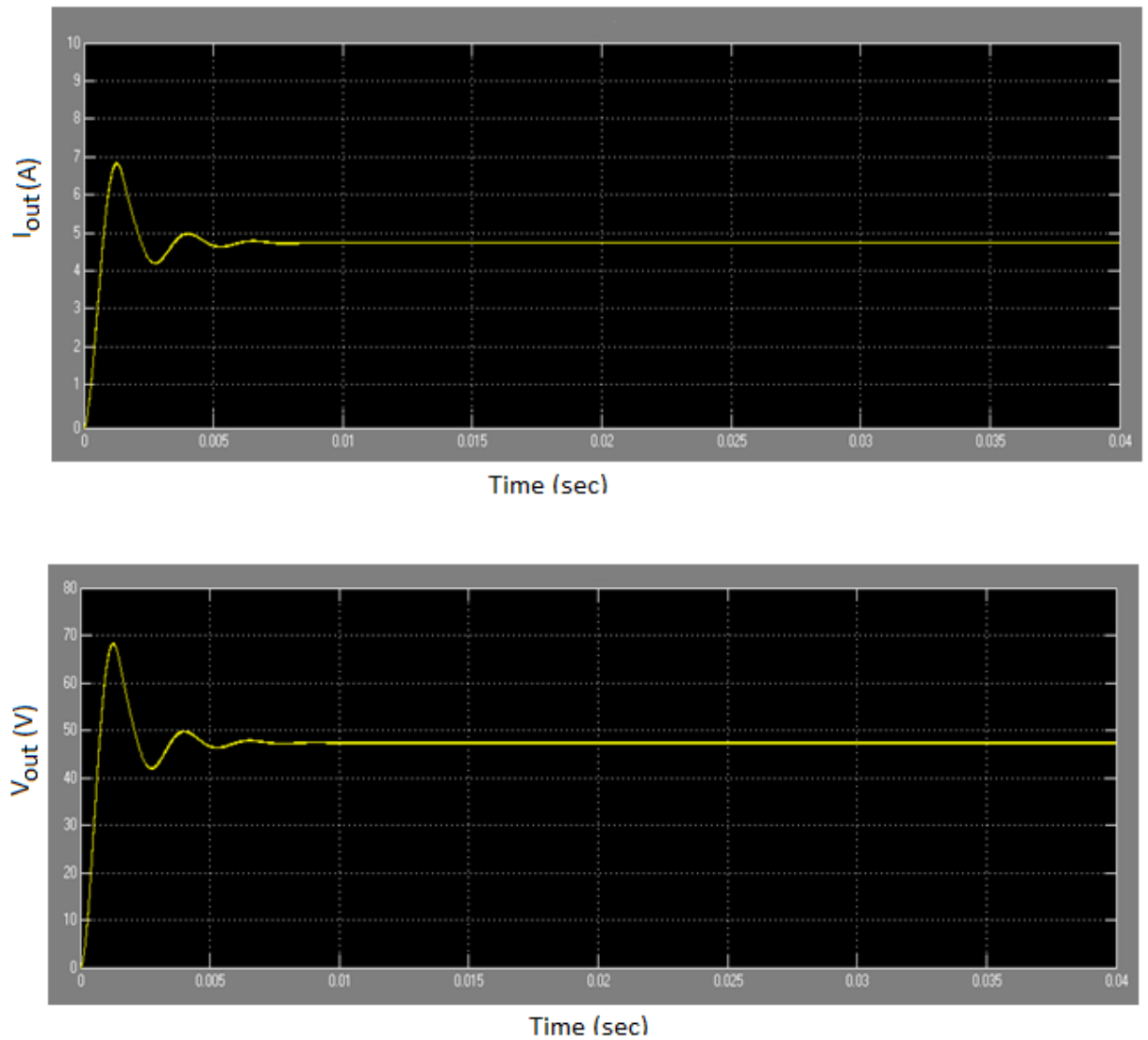

Figure 4.1 Simulated Waveforms of a Low Voltage DC-DC Boost Converter

4.2 Simulation Results of the Integrated Model

As the design process was divided into three steps, three corresponding simulation results occurred. The following section provides simulation results separately.

4.2.1 Simulation results of the medium voltage DC-DC Converter

Results for this specific design of medium voltage DC-DC converter were obtained using the Simulink and are presented in Figure 4.2. As shown, simulated results are in close agreement with expected theoretical results. The input voltage is 400 V and expected output voltage at the output terminal of the circuit was 4150 V.

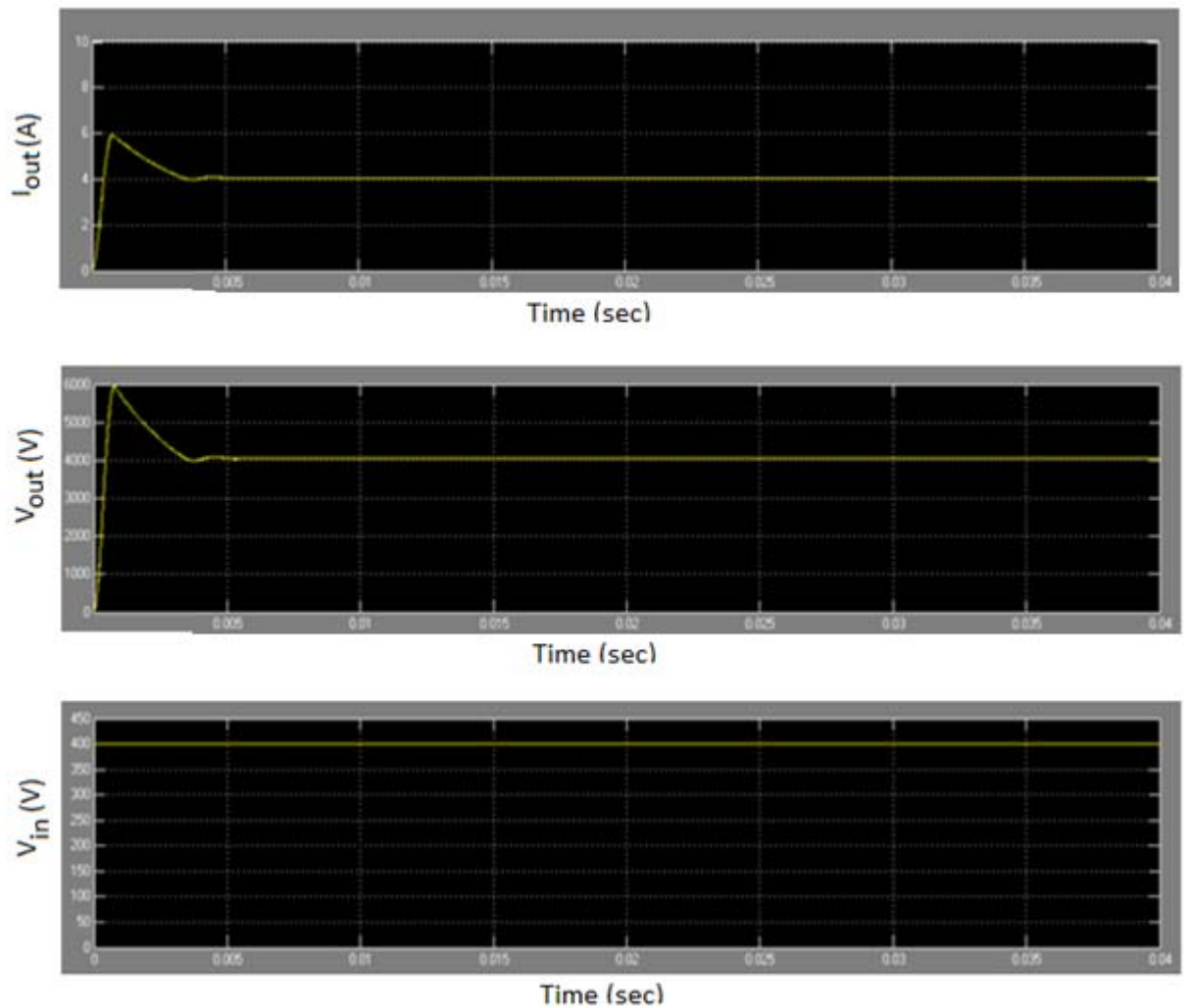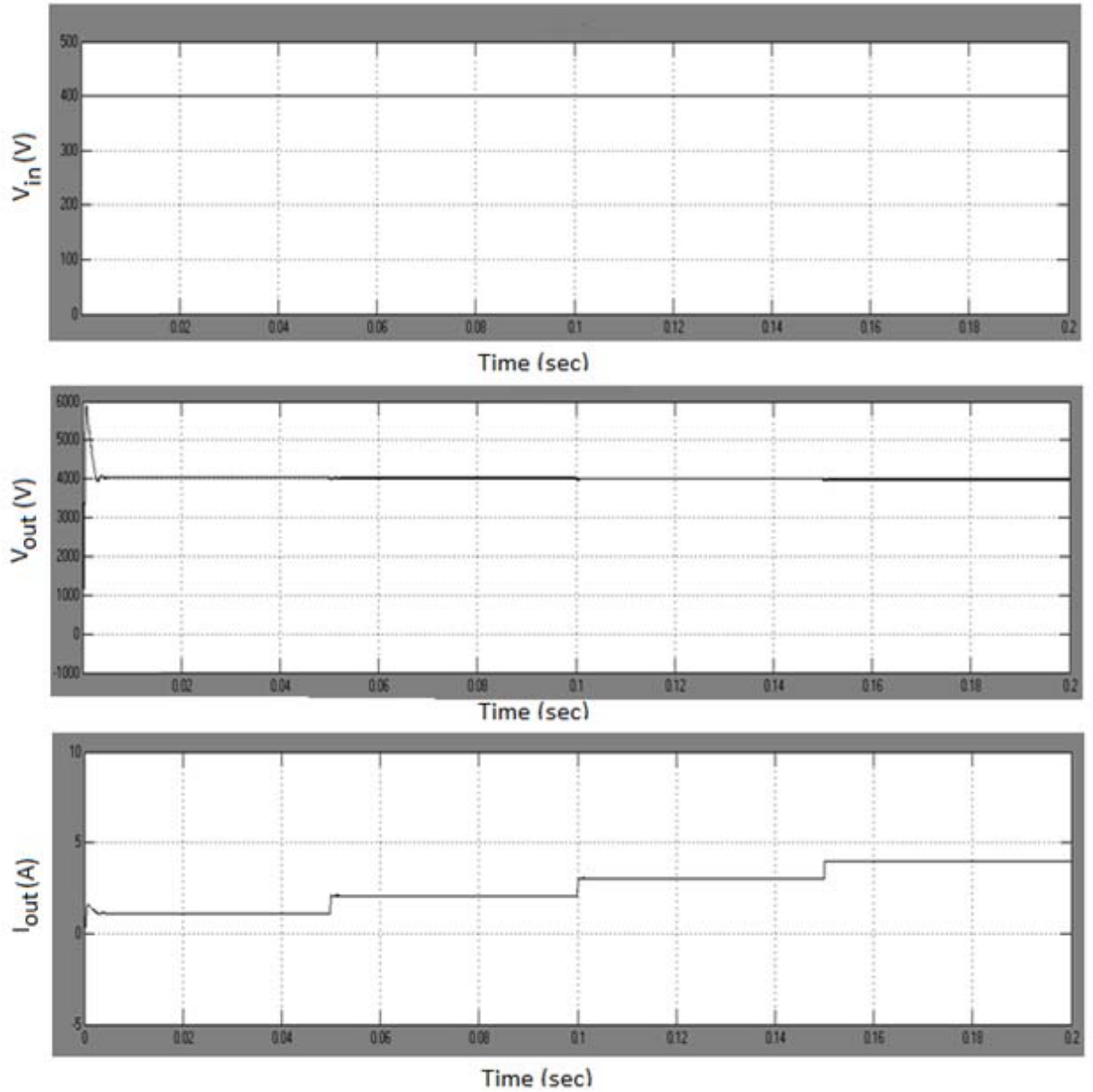**Figure 4.2 Simulated Waveforms of a Medium Voltage DC-DC Boost Converter**

4.2.2 Simulation results of the medium voltage DC-DC Converter and load

Simulation results of the Simulink model after connecting the DC-DC converter to a load is shown below. Figure 4.3 shows; that the desired output voltage (4150 V) is obtained.

Figure 4.3 Simulated Waveforms of a DC-DC Boost Converter and Load

4.2.3 Simulation results of the medium voltage DC-DC Converter, Battery and load

The final simulation corresponds to the Simulink model of the combination of battery, DC-DC converter and load. As seen from the simulation results of Figure 4.4, desired output voltage of approximately 4150 V is again obtained.
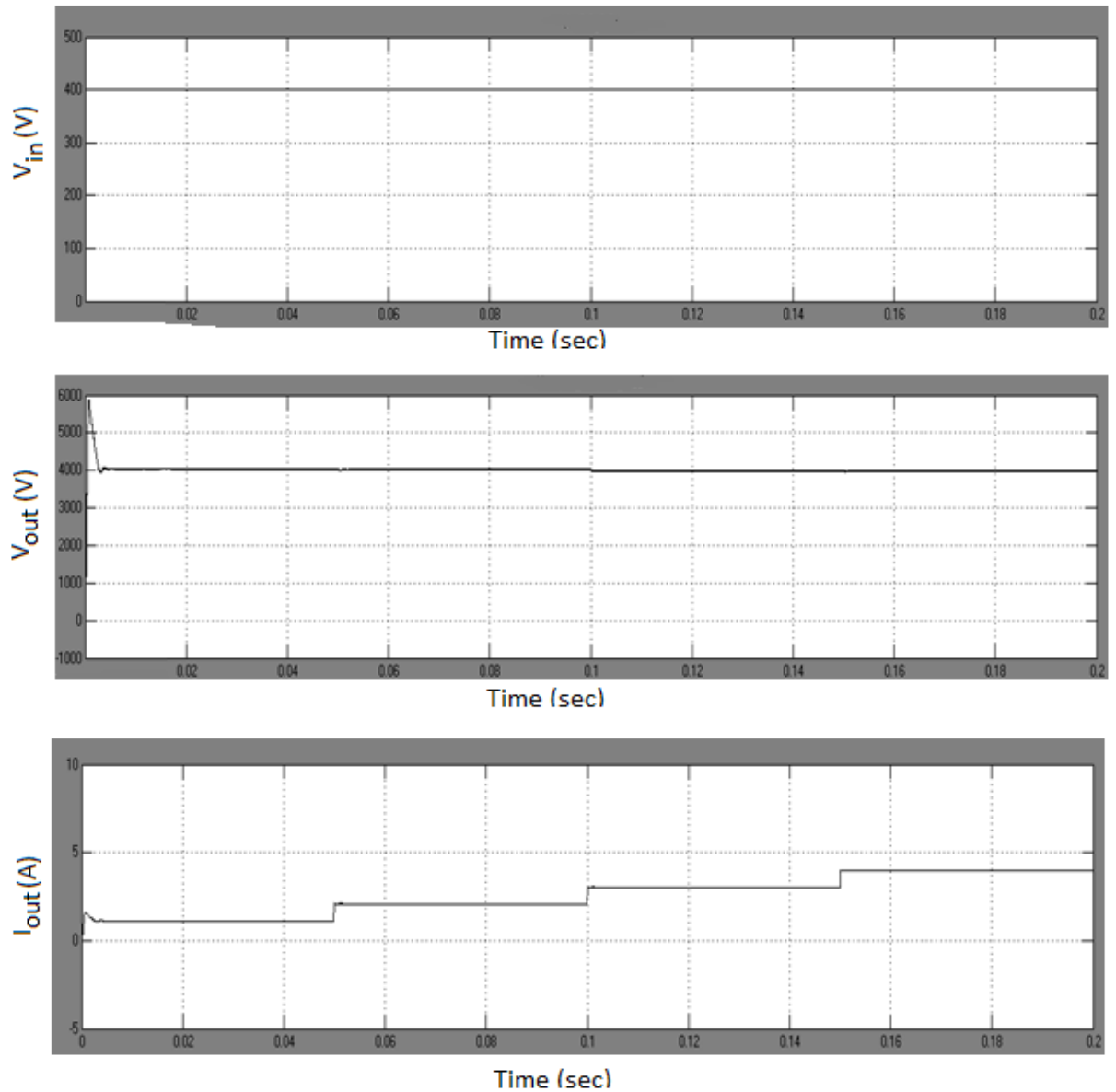

Figure 4.4 Simulated Waveforms of a Battery, Converter and Load

4.3 Summary

This section provided simulation results of Matlab/Simulink models of a low voltage DC-DC boost converter and a medium voltage DC-DC boost converter. Designs of the converters differ slightly from each other and distinctive assumptions were considered for each design. Based on designed models in this study, simulation results are obtained and analyzed. As it can be observed from the simulation results of voltage and current, a transient occurred for few seconds. First, a low voltage DC-DC converter was designed, and its simulation result matched the desired level of output voltage. Next, a simulation result was found by designing a medium voltage DC-DC converter, and the result was in agreement with expected output voltage. Then, a load modeled in Simulink was connected with the converter and its simulation result was provided, yet it matched with the desired output voltage. Finally, the battery, converter and load were combined as one model and the simulation result was obtained, matching the desired objectives in terms of output voltage.

Chapter 5. Conclusion and Future Work

DC-DC converters and their design remain as an interesting topic. The main objectives of the report were to verify a previously designed battery model, design a medium voltage DC-DC boost converter and load in Matlab/Simulink, and design a single model that contains the battery, converter and load. The battery, converter and load were separately designed and later combined in to one model. Their simulation result is provided and analyzed.

The theoretical back ground of converters and design of boost converter are discussed in detail. It was found that the output voltage depends on many parameters but mainly on the switching frequency, duty ratio and values of inductance and capacitance of the inductor and capacitor respectively. Selection of the parameters was accomplished so that the desired output voltage would be obtained. In all the results, transients occurred for few seconds before settling at the desired output.

One possible extension of this report is to incorporate a proportional-integral-derivative controller (PID controller) with the DC-DC converter [22]. Usually, PID controller is useful in determining the 'error' value between a measured process variable and a desired setpoint, thereby minimizing the error by adjusting the input. This extension may be able to improve the performance of the battery.

References

[1]   J. Billo, "Models and Methods for Shipboard Power System Reconfiguration", *Msc Thesis for University of Texas*, 2003.

[2]   Karen L. Butler-Purry and N.D.R Sarma, "Visualization for Shipboard Power Systems", *Proceedings of the 36th Hawaii International conference on System Sciences,* 2003.

[3]   B. Kennedy, D. Patterson and S. Camilleri, "Use of Lithium-ion Batteries in Electric Vehicles", *Journal of Power Sources*, vol. 156, pp. 541 -546, 2006.

[4]   Jinbo Wu, Jinyu Wen, Haishun Sun, and Shijie Cheng, "A Novel Energy Storage System based on Flywheel for Improving Power System Stability", *Journal of Electrical Engineering and Technology,* vol. 6, No. 4, pp. 447-458, 2011.

[5]   N. Mohan, T. Undeland, W. Robbins, *Power Electronics: Converters, Applications and Design*, ISBN 0-471-61342-8, 1989.

[6]   S. A. Khateeb, M.M. Farid, J.R Selman and S. Al-Hallaj, "Mechanical-electrochemical modeling of Li-ion Battery Designed for an Electric Scooter", *Journal of Power Sources*, vol. 158, pp 673-678, 2006.

[7]   Lijuan Gao et al, "Dynamic lithium-ion Battery Model for System Simulation", *IEEE Transactions on Components and Packaging Technologies*, vol. 25, No. 3, pp. 495-505, 2004.

[8]   M.Chen and G.A.R Mora, "Accurate Electrical Battery Model Capable of Predicting Runtime and I-V Performance", *IEEE transactions on Energy Conversion*, vol. 21, pp. 504-511, 2006.

[9]   O. Erdinc et al, "A dynamic lithium-ion Battery Model Considering the Effects of Temperature and Capacity Fading", *Conference Publication on Power Sources,* pp. 383-386, 2009.

[10]   D.H. Doughty, P.C. Butler, R. G. Jungst and E.P. Roth, "Lithium Battery Thermal Models", *Journal of Power Sources,* vol. 110, pp. 357-363, 2002.

[11]   S.C.Chen, C.C Wan and Y.Y Wang, "Thermal Analysis of Lithium-ion Batteries", *Journal of Power Sources*, vol. 140, pp. 111-124, 2005.

[12]   S.S. Zhang, K. Xu and T.R. Jow, "Study of the Charging Process of a LiCoO2-based Li-ion battery", *Journal of Power Sources*, vol. 160, pp. 1349-1354, 2006.

[13]   S.S. Zhang, K. Xu and T.R. Jow, "Charge and Discharge Characteristics of a Commercial LiCoO2-based 18650 Li-ion Battery", *Journal of Power Sources*, vol. 160, pp. 1403-1409, 2006.

[14]   Santosh Hariharan and V.Naveen Kumar, "Design of a DC-DC Converter for a PV Array", *International Conference on Industrial Electronics*, pp. 79-84, 2010.

[15]   J.W. Kimball, T.L. Flowers, P.L. Chapman, "Issues with Low-input-voltage Boost Converter Design", IEEE 35th Annual Conference, vol. 3, pp. 2152-2156, 2004.

[16]   P.Sanjeevikumar and K. Rajambal,"Extra-high-voltage DC-DC Boost Converters Topology with Simple Control Strategy", *Hindawi Publishing Corporation*, vol. 2008, 2008.

[17]   Athimulam Kalirasu et al, "Simulation of Closed Loop Controlled Boost Converter for Solar Installation", *Serbian Journal of Electrical Engineering*, vol. 7, pp. 121-130, 2010.

[18]   Emad M. Ahmed et al, "On the Behavior of Marine and Tidal Current Converters with DC-DC Boost Converter", *IEEE International Power Electronics and Motion Control Conference*, pp. 2250-2254, 2012.

[19]   K. Prabakaran et al, "DC-DC Boost Converter Topologies for High Voltage Applications", P*roceedings of the National Conference on Trends in Instruments and System Design Automation*, 2007.

[20]   G. Hua, E.X. Yang et al, "Novel zero-current transition PWM converters", *IEEE Transition in Power Electronics*, vol. 9, No. 6, pp. 601-606, 1994.

[21]   J. Newman, K.E. Thomas, H. Hafezi and D.R. Wheeler, "Modeling of Lithium-ion Batteries", *Journal of Power Sources*, vol. 119-121, pp. 838-843, 2003.

[22]   S.M.R Rafiei, R. Ghazi, R. Asgharian, M. Barakati, and H.A. Toliyat, "Robust control of DC-DC PWM converters: A comparison of H_inf, Miu, and Fuzzy Logic Based Approaches", P*roceedings of the IEEE 2003 Control Applications Conference*, vol. 1, pp. 603-608, 2003.